Biochimica et Biophysica Acta 1788 (2009) 666–675

Contents lists available at ScienceDirect

Biochimica et Biophysica Acta

journal homepage: www.elsevier.com/locate/bbamem

Membrane microdomains: Role of ceramides in the maintenance of their structure and functions

Galya Staneva [a,*], Albena Momchilova [a], Claude Wolf [b], Peter J. Quinn [c], Kamen Koumanov [a,*]

[a] Institute of Biophysics, Bulgarian Academy of Sciences, Acad. G. Bonchev Str., Bl.21, 1113 Sofia, Bulgaria
[b] Universite Paris 6, INSERM U538, CHU St. Antoine, 27 rue Chaligny, 75012 Paris, France
[c] Biochemistry Department, King's College London, 150 Stamford Street, London SE1 9NH, UK

ARTICLE INFO

Article history:
Received 4 September 2008
Received in revised form 13 October 2008
Accepted 29 October 2008
Available online 13 November 2008

Keywords:
Ceramide
Cholesterol
Sphingomyelin
Raft
Sphingomyelinase
Phospholipase A_2
GUV
Lipid signaling pathway

ABSTRACT

Free-standing giant unilamellar vesicles were used to visualize the complex lateral heterogeneity, induced by ceramide in the membrane bilayer at micron scale using C_{12}-NBD-PC probe partitioning under the fluorescence microscope. Ceramide gel domains exist as leaf-like structures in glycerophospholipid/ceramide mixtures. Cholesterol readily increases ceramide miscibility with glycerophospholipids but cholesterol–ceramide interactions are not involved in the organization of the liquid-ordered phase as exemplified by sphingomyelin/cholesterol mixtures. Sphingomyelin stabilizes the gel phase and thus decreases ceramide miscibility in the presence of cholesterol. Gel/liquid-ordered/liquid-disordered phase coexistence was visualized in quaternary phosphatidylcholine/sphingomyelin/ceramide/cholesterol mixtures as occurrence of dark leaf-like and circular domains within a bright liquid phase. Sphingomyelin initiates specific ceramide–sphingomyelin interactions to form a highly ordered gel phase appearing at temperatures higher than pure ceramide gel phase in phosphatidylcholine/ceramide mixtures. Less sphingomyelin is engaged in formation of liquid-ordered phase leading to a shift in its formation to lower temperatures. Sphingomyelinase activity on substrate vesicles destroys micron L_o domains but induces the formation of a gel-like phase. The activation of phospholipase A_2 by ceramide on heterogeneous membranes was visualized. Changes in the phase state of the membrane bilayer initiates such morphological processes as membrane fragmentation, budding in and budding out was demonstrated.

1. Introduction

Ceramides are relatively minor constituents of animal cell plasma membranes [1]. Attention has been focused more recently on ceramides as their mediator functions in different cellular processes are recognized functions [2–4]. Ceramide (CER) molecules form specific membrane domains which can exist in gel phase (L_β) within domains of liquid-ordered phase (L_o) [5,6]. Cell CER is either synthesized *de novo* [7] or originates as a product of hydrolysis of sphingomyelin (SM) by sphingomyelinase [8]. Membrane-bound sphingomyelinases have been reported to be localized predominantly in membrane raft domains [9], implying that CER produced by the action of sphingomyelinases formed from substrate present in these domains [10,11].

CER are hydrolytic products of SM but the two lipids have different affinities for other lipid components of membranes especially cholesterol. SM and cholesterol (CHOL) form L_o phase (lipid matrix of cellular rafts), whereas CER destabilizes these phases, displacing CHOL from the favorable SM/CHOL interactions [12] and usually segregates into CER-enriched domains [13–15]. The formation of CER-enriched gel structures in a mixture containing other phospholipids can be explained by the strong inter-molecular interactions between the CER molecules, thus forming a compact membrane structure. We recently reported that SM can also be a component of this gel phase [16]. The stability of CER/SM interactions is evident from the persistence of highly ordered structures probed by electron spin resonance (ESR) spectroscopy and the appearance of a sharp wide-angle X-ray reflection at temperatures higher than the gel–fluid transition of CER alone in egg phosphatidylcholine bilayers. The formation of gel phases in binary mixtures of CER and SM has also been reported by other workers [17].

Accumulation of CER in plasma membranes basically induces significant structural alterations in the membrane bilayer. CER in membranes have been shown to perform a very fast flip-flop with half-times ranging from several seconds [18,19] to minutes [19,20]. In addition, the CER formed in the membrane as a product of sphingomyelinase activity, have been shown to induce transmembrane translocation of other membrane phospholipid components, which results in disappearance of their asymmetric distribution [21].

* Corresponding authors. G. Staneva is to be contacted at Tel.: +35929793686; fax: +35929712493. K. Koumanov, Tel.: +35929792623; fax: +35929712493.
E-mail addresses: gstaneva@obzor.bio21.bas.bg, g_staneva@yahoo.com (G. Staneva), koumanov@obzor.bio21.bas.bg (K. Koumanov).

0005-2736/$ – see front matter © 2008 Elsevier B.V. All rights reserved.
doi:10.1016/j.bbamem.2008.10.026

This property of CER molecules suggests involvement in the CER-related mechanisms of cell signaling. By forming membrane microdomains, CER molecules induce structural defects in the membrane bilayer which favor the activity of certain lipolytic enzymes. For example, we reported that CER incorporated into model phospholipid membranes or generated as a result of sphingomyelinase activity induces a strong activation of phospholipase A_2, whereas the substrate SM decreases its activity under similar circumstances [22].

In our recent paper we determined the structure, thermotropic phase behavior, dynamic motion and order parameters of bilayer dispersions containing egg phosphatidylcholine (EPC), egg sphingomyelin (ESM), egg ceramide (ECER) and CHOL [16]. The coexistence of gel, liquid-ordered and liquid-disordered structures has been determined in phosphatidylcholine/ceramide/sphingomyelin/cholesterol mixtures by peak fitting analysis of synchrotron X-ray powder patterns. Molecular order parameters have been derived from the motion of spin-label probes using spectral simulation methods.

In the present studies, fluorescence microscopy of giant unilamellar vesicles (GUVs) prepared from lipid mixtures examined previously by biophysical methods (X-ray and ESR) has been used to visualize the formation and destabilization of L_o and L_β phases induced by CER. We observed changes in L_o domain formation, size and dynamics as a function of the proportion of CER in the bilayer and temperature of binary, ternary and quaternary mixtures. We observed how a heterogeneous membrane structure, with lateral domains in the membrane on a micron scale, are able to modulate sphingomyelinase and phospholipase A_2 activity, enzyme-mediated vesicle transformations and, vice versa, how enzyme activity could reorganize the coexisting phases. We focused our attention on phospholipase A_2 and sphingomyelinase, because of the known implication of these enzymes in cell signaling processes.

2. Materials and methods

2.1. Commercial reagents

Lipids were obtained from Sigma-Aldrich, St Quentin-Fallavier, France and used without further purification as follows: egg-yolk L-α-phosphatidylcholine, egg-yolk sphingomyelin, egg-yolk ceramide and cholesterol. The distribution of fatty acids in egg phosphatidylcholine consisted of 34% C16:0, 2% C16:1, 11% C18:0, 32% C18:1, 18% C18:2 and 3% C20:4 and for egg sphingomyelin and ceramide it was 84% C16:0, 6% C18:0, 2% C20:0, 4% C22:0 and 4% C24:0. The enzymes sphingomyelinase (*Staphylococcus aureus*; 20 U/ml; specific activity 100–300 U/mg protein in 0.5 mM Hepes buffer, pH 7.4 and 5 mM $MgCl_2$) and secretory phospholipase A_2 (sPLA$_2$) (Bee venom — *Apis mellifera*; 1000 U/ml; specific activity 1360 U/mg protein in 0.5 mM Hepes buffer, pH 7.4 and 10 mM $CaCl_2$) were also purchased from Sigma-Aldrich. The fluorescent lipid analogue C_{12}-NBD-PC was purchased from Avanti Polar Lipids, Alabaster, AL.

2.2. Preparation of giant unilamellar vesicles

GUVs were prepared using an electroformation method developed by Angelova and Dimitrov [23]. Binary, ternary and quaternary mixtures of EPC, ECER, ESM and CHOL were prepared in the required lipid molar ratios. GUVs were formed in a temperature-controlled chamber mounted on a Peltier microscope stage in which the rate of temperature change was 0.2°/min. The protocol for formation of unilamellar giant heterogeneous vesicles was as described in Staneva et al. [24]. GUVs were prepared in a buffer of 0.5 mM Hepes, pH 7.4. The vesicles were invariably formed at temperatures above the phase transition temperature for given mixtures or the growth temperature was chosen to be the maximal temperature at which a high yield of vesicles was consistently obtained. Although deposited lipids are uniformly mixed, each vesicle varied slightly in composition, reported by Veatch et al. [25]. This could be observed as different miscibility transition temperatures and brightness between vesicles reflecting uneven dye distribution. This composition error is estimated to be ≅2%. The chain-labeled lipid analogue PC-NBD is excluded from the more ordered phase and partitions predominantly in the disordered phase. Thus the more ordered phase appears as a dark spot within the bright vesicle membrane.

2.3. Microinjection of enzymes

Picoliter aliquots of sphingomyelinase and secretory phospholipase A_2 were applied to the outer surface of individual giant vesicles. The micro-injection was carried out with an Eppendorf Transjector 5246. Micropipettes with inner tip diameters of 1–2 μm were made of borosilicate capillaries (1.2 mm outer diameter) by a microprocessor-controlled vertical puller (PC-10, Narishige). A detailed study of the influence of injection parameters was initially performed with buffer in control experiments to define the range of injection pressures, times and distance that resulted in the least perturbation of the shape of the vesicle during the injection. Injections were performed from a distance of about 30–50 μm from the vesicles. Injected volumes of concentrated enzyme stock solution were of the order of a few picoliters. It should be noted that the precise volume injected is not known but is reproducible as a function of injection pressure and time and can be varied proportionally by varying the injection time. The observations presented below are based on results obtained from at least 5–10 duplicate experiments.

2.4. Video microscopy

The vesicles were observed using a Zeiss Axiovert 135 microscope, equipped with a 40× long working distance objective lens (LD Achroplan Ph2). The observations were recorded using Hamamatsu B/W chilled CCD camera (C5985-10) connected to an image recording and processing system. The phase morphology transformations of the heterogeneous GUV membranes were followed in phase contrast and

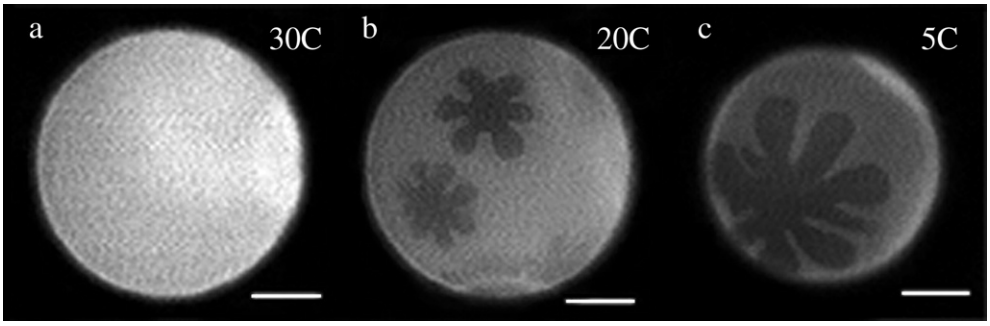

Fig. 1. Visualization of L_β/L_d phase separation in ceramide-containing GUVs at the microscopic scale. EPC/ECER 80/20 mixture yields homogeneous vesicles from 37 °C to 30 °C (a). Well resolved dark leaf-like domains at 20 °C (b) and their growth in size are observed with decreasing temperature (c). Bar 20 μm.

in fluorescence by Zeiss filter set 16 (Ex/Em=485/>520 nm). For the micromanipulation of the vesicles, a micromanipulator from Narishige MMN-1 plus MMO-22 equipped with a joy-stick and an Eppendorf microinjector was used.

3. Results

3.1. GUVs prepared from egg yolk phosphatidylcholine/ceramide binary mixtures (EPC/ECER)

To visualize gel (L_{β})/liquid (L_d) phase separation, single GUVs composed of EPC/ECER (90/10, data not shown) and (80/20, Fig. 1) were observed in the temperature range from 4° to 37 °C. Upon cooling, from 37° to 30 °C the vesicles exhibited a homogeneous appearance whereas below 30 °C two different regions were clearly resolved as evident from the fluorescence images at the microscopic scale. The formation of dark domains is a consequence of the exclusion of PC-NBD from the ordered phase and its partition into the remaining L_d phase, appearing as a bright phase [26,27]. The dark regions formed leaf-like domains which were observed to float laterally within the plane of the bright lipid phase. The number of petals in the leaf-like domains was usually six or eight. In accordance with the X-ray data, EPC/ECER binary mixtures exhibit gel/liquid phase coexistence in the temperature range 2–42 °C which is consistent with the presence of the dark leaf-like domains, enriched in CER in gel state [16]. These gel-state domains typically do not fuse to yield a larger domain as usually observed for L_o/L_d phase separation [28]. It is noteworthy that phase separation cannot be ruled out in the uniformly appearing vesicles. There are two possible reasons for the above observation. The first possibility is that phase separation consists of domains of a nanometer scale dimension. This hypothesis is plausible in view of the fact, that the gel phase signature in the WAXS (wide angle X-ray scattering) region was detected at temperatures up to 42 °C in this mixture. The second possibility is that the partition coefficient of the fluorescent lipid analogue in the two phases tends to coincide at higher temperatures. For example, dark leaf-like domains were hardly resolved in the temperature range 32 °–25 °C due to the low contrast between two coexisting phases but were well resolved at temperatures around 20 °C.

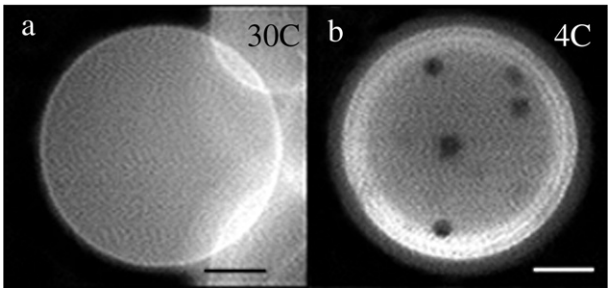

Fig. 3. L_{β}/L_d phase separation in a ternary EPC/ECER/CHOL 60/10/30 mixture. Uniform appearance is detected from 37 °C to 5 °C (a). Formation of dark domains is observed below 5 °C (b). Domain boundaries are not sharply resolved. Bar 20 μm.

3.2. GUVs prepared from egg yolk phosphatidylcholine/ceramide/cholesterol ternary mixtures (EPC/ECER/CHOL)

3.2.1. EPC/ECER/CHOL 80/10/10

The equimolar ratio between CHOL and CER in EPC/ECER/CHOL 80/10/10 ternary mixture (Fig. 2a–c) did not significantly change the scenario of leaf-like domain formation observed in binary mixtures. However, a larger number of smaller domains were observed at low temperatures (Fig. 2e, f). The petals were more elongated and with a finer base (Fig. 2f) compared with the binary mixture (EPC/ECER 80/20). Phase contrast images demonstrated a lack of outward or inward budding at the domain location (Fig. 2d) as previously observed for L_o/L_d phase separation [29,30].

3.2.2. EPC/ECER/CHOL 70/10/20

At 20% CHOL the formation of the leaf-like domains was shifted down by 10° compared with those of the EPC/ECER/CHOL 80/10/10 mixture. The leaf-like domains were detected at temperatures below 10 °C.

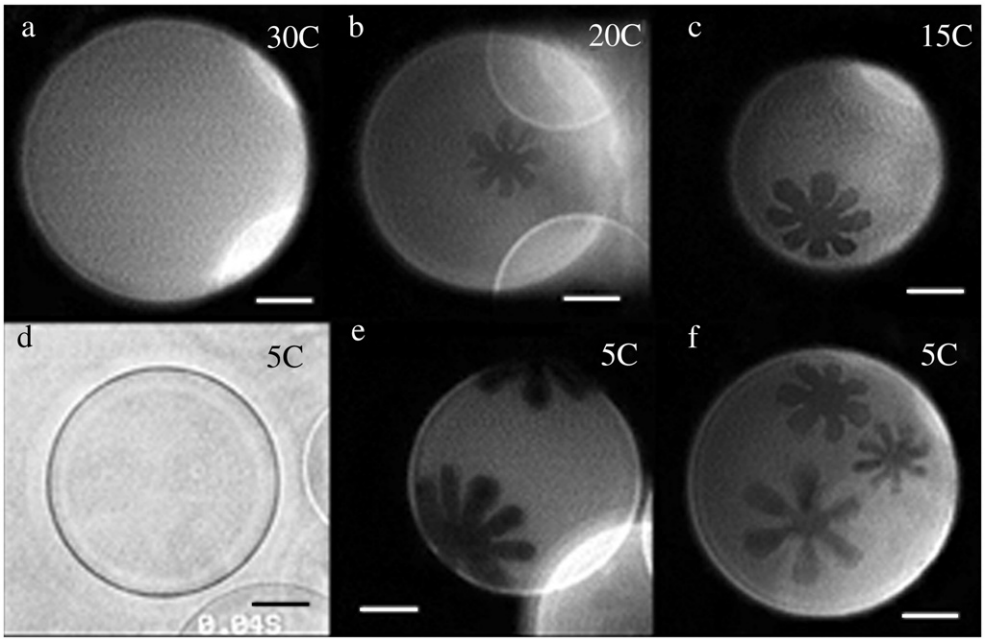

Fig. 2. L_{β}/L_d phase separation in EPC/ECER/CHOL 80/10/10 ternary mixture. Uniform appearance is detected from 37 °C to 30 °C (a). Formation and growth in size of dark leaf-like domains is observed in images *b* and *c*. The phase contrast observation shows no outward or inward budding of domain location (d). A larger number of domains is seen at low temperatures (e and f) compared to the binary mixture. The petals are characterized by a more elongated shape and finer attachment to the central area of the domains (f) compared to the EPC/ECER 80/20 binary mixture. Bar 20 μm.

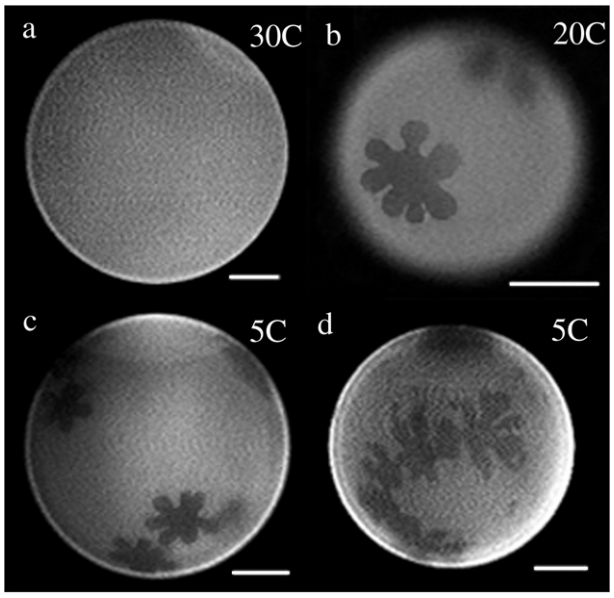

Fig. 4. L_β/L_d phase separation in a quaternary EPC/ESM/ECER/CHOL 75/5/10/10 mixture. Formation of irregular leaf-like domains and clustering of domains is evident *(c* and *d)*. Bar 20 μm.

3.2.3. EPC/ECER/CHOL 60/10/30

At 30% CHOL, the vesicles remained with a homogeneous appearance in a wide temperature range from 37 °C to 5 °C (Fig. 3a). Dark domains appeared below 5 °C and the shape of the domains was not clearly resolved. It was not possible to establish whether domains were round or leaf-like in shape but during 30 min of observation at 4 °C these domains did not grow in size by fusion. Therefore, these domains could be assigned as gel phase.

3.3. GUVs prepared from egg-yolk phosphatidylcholine/sphingomyelin/ceramide/cholesterol quaternary mixtures (EPC/ESM/ECER/CHOL)

The subcellular localization of ceramide molecules in plasmalemmal microdomains (caveolae and rafts), lysosomes and mitochondria represents a key factor which determines their cellular function [31]. Ceramide might be transferred from endoplasmic reticulum to the Golgi apparatus and mitochondria by membrane contacts between these cellular compartments. Some of these compartments are poor and others are enriched in cholesterol. That justifies our studies of the impact of ceramide on phase separation in two different series of quaternary mixtures: CHOL-poor (10%) and CHOL-enriched (20%).

3.3.1. EPC/ESM/ECER/CHOL 75/5/10/10

The addition of SM to the quaternary mixtures altered the regular pattern of the leaf-like gel domains (Figs. 4–7). Addition of only 5% SM induced formation of more irregular domains (Fig. 4) indicating a tendency to attach to each other. As a result, clusters comprised of two or more attached domains were seen to move together on the membrane surface (Fig. 4c and d).

3.3.2. EPC/ESM/ECER/CHOL 70/10/10/10

Addition of more SM resulted in an increase of the number of petals and in the extension of the area, where petals attach at low temperatures (Fig. 5a–c). The phase contrast image of L_β/L_d phase separation in the EPC/ESM/ECER/CHOL 70/10/10/10 quaternary mixture (Fig. 5b) revealed a defect in the curvature of the bilayer corresponding to the location of the gel domains detected by fluorescence (Fig. 5a). Clearly resolved leaf-like domains were observed in all temperature range from 20° to 5 °C as well as in binary mixtures.

3.3.3. EPC/ESM/ECER/CHOL 60/20/10/10

L_β/L_d and $L_\beta/L_o/L_d$ phase coexistence was observed in this quaternary mixture between 20 ° and 5 °C and below 5 °C, respectively. The coexistence of two different dark domains at very low temperatures (leaf-like and circular) is shown in Fig. 6. The small circular domains were assigned as liquid-ordered phase. The liquid-ordered domains are characterized by their circular shape and a large number of small domains at the miscibility transition. The assignment of a perfectly round shape is difficult due to the small size of these domains and the weak contrast between bright and dark regions. An argument to explain the observed images can be the quasi-equal value of the L_o/L_d partition coefficient. However, the formation of multiple domains at 4 °C (Fig. 6b) which grow in size by fusion (Fig. 6c) seems to be an intrinsic property of liquid-ordered domains.

3.3.4. EPC/ESM/ECER/CHOL 50/30/10/10

30% SM decreased the number of petals to only two or three at 15 °–20 °C (Fig. 7a and b). At low temperatures (2–10 °C) the extension of the central area of the domain was dominant with respect to the area of the petals (Fig. 7c). The dark leaf-like domains displayed a more rounded shape. In some cases the dimension of the petals was so small that they appeared as tiny protrusions on the edge of the dark domain. The visualization of the phase separation was impeded at low temperatures because of the vesicle shrinkage. It is likely that the gel fraction was so abundant that the membrane elasticity was reduced to a point where the vesicles were not stable.

3.3.5. EPC/ESM/ECER/CHOL 60/17.5/5/17.5

Increasing the proportion of CHOL to 17.5% provides a more realistic model of the outer leaflet of cellular plasma membranes. In

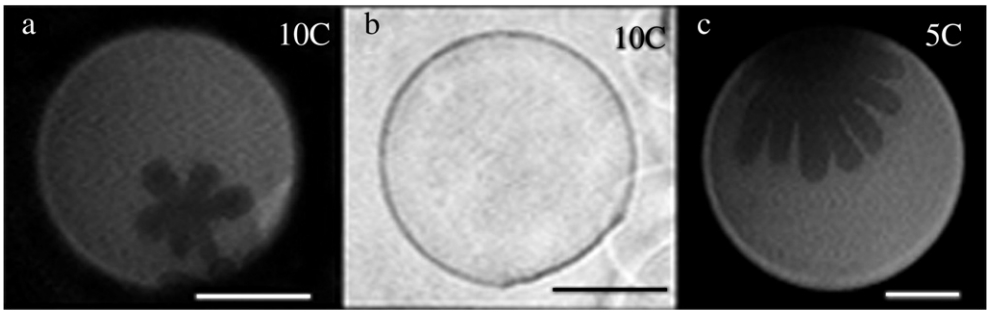

Fig. 5. L_β/L_d phase separation in a quaternary EPC/ESM/ECER/CHOL 70/10/10/10 mixture. Irregular leaf-like shape of the domains characterized by an increased number of petals and an extended central area was observed (a and c). Phase contrast image (b) shows the defect in the curvature corresponding to the domain location in the equatorial section (a). Bar 20 μm.

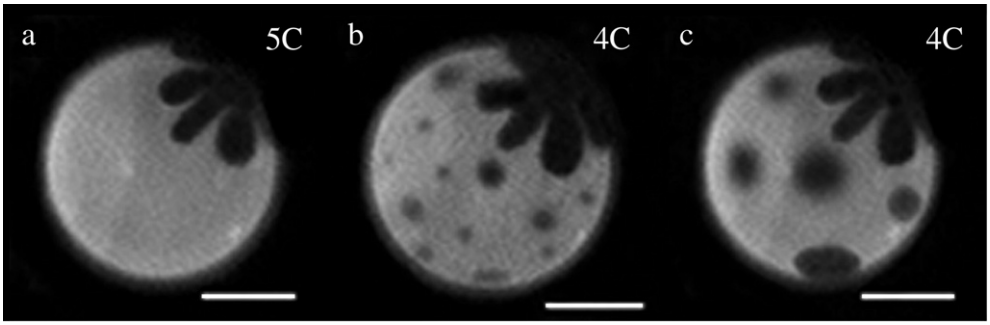

Fig. 6. Phase separation in a quaternary EPC/ESM/ECER/CHOL 60/20/10/10 mixture. L_{β}/L_d phase coexistence is evident at 5 °C (a). $L_{\beta}/L_o/L_d$ phase coexistence is observed below 5 °C in the course of L_o domain formation (b) and fusion (c). Bar 20 μm.

the absence of CER the tertiary mixture EPC/ESM/CHOL 65/17.5/17.5 exhibited formation of L_o/L_d phase separation around 20 °C. The vesicles varied slightly in composition and a miscibility transition was observed between 24° and 20 °C. Below these temperatures the liquid-ordered phase coexisted with a bright L_d phase in the form of a number of dark and small circular domains. The average size of domains was of the order of a few micrometers (Fig. 8a). The addition of only 5% to 10% CER induced a shift of the L_o/L_d phase separation to higher temperatures by about 10°C. Thus, at 20 °C the dark areas assigned to the L_o fraction were more expanded (Fig. 8b) and this expansion was not only due to simply addition of 5% sphingolipid. For example, a clear difference in the area of the dark fractions (Fig. 8c) was detected between the control EPC/ESM/CHOL 60/22.5/17.5 ternary mixture (Fig. 8c), composed only of SM and this quaternary mixture where the sphingolipid ratio was 17.5% SM and 5% CER (Fig. 8b). Dark areas in the control mixture did not occupy more than one quarter of the vesicle area compared to the CER-enriched mixture. Possibly, the CER molecule participated in the dark domains. Leaf-like domains were not observed in mixtures of these lipid ratios.

3.3.6. EPC/ESM/ECER/CHOL 50/17.5/15/17.5

15% CER added to a quaternary mixture resulted in formation of irregular dark domains at the phase transition temperature where the appearance of the membrane became more heterogeneous (Fig. 9a). There was apparently a threshold ratio of ESM/ECER (roughly 1 to 1) which dramatically changed the scenario of phase separation at 20 °C. The leaf-like domains were preferentially formed in these proportions of ESM and ECER at 20 °C whereas the formation of dark circular domains was shifted down to 15 °C (Fig. 9c). At lower temperatures (6 °C) the phase morphology of the membrane bilayer was reorganized and the formation of band-like dark domains was observed (Fig. 9d).

3.3.7. EPC/ESM/ECER/CHOL 45/17.5/20/17.5

With 20% CER, at 10°C the extension of the bright/dark areas was reversed. The formation of a large number of small bright domains was observed contrasting on a dark background (Fig. 10a), a process known as phase percolation. The leaf-like domains cannot be visualized for this phase distribution since the dark phase was dominant and L_{β}/L_o contrast is insufficient. Bright domains fused to form one or two large bright regions separated by a dark band at low temperatures (Fig. 10b). However, in particular cases, the detection of leaf-like domains was possible when gel domains were large enough and were located at the L_o/L_d phase border as was demonstrated in Fig. 10b. Usually, the fluorescence time exposures for visualization of L_o/L_d phase coexistence would be two to three times less than L_{β}/L_o due to the greater PC-NBD coefficient of partition in L_o/L_d phases. However, if we admit the existence of phase separation in the dark region, then the contrast would not be sufficient to visualize L_{β}/L_o coexistence on the L_d background. In some cases, as mentioned above, three-phase coexistence was possible at favorable three-dimensional configuration of phases. This is consistent with the report of Chiantia et al. [5] who identified a third topographical level by atomic force microscopy, being almost 0.4 nm higher than the liquid-ordered phase. Interestingly, these new domains are always localized in SM-rich domains, either in the interior or at the domain boundaries. This membrane organization is not surprising because it is the most energetically favorable lipid arrangement: gradient in membrane thickness in order to avoid unfavorable hydrophobic mismatch.

3.4. Sphingomyelinase activity in L_o/L_d heterogeneous membranes

To study the consequences of the enzymic conversion of SM into CER in a heterogeneous membrane which presents L_o/L_d phase separation at the micrometric scale we treated model membrane

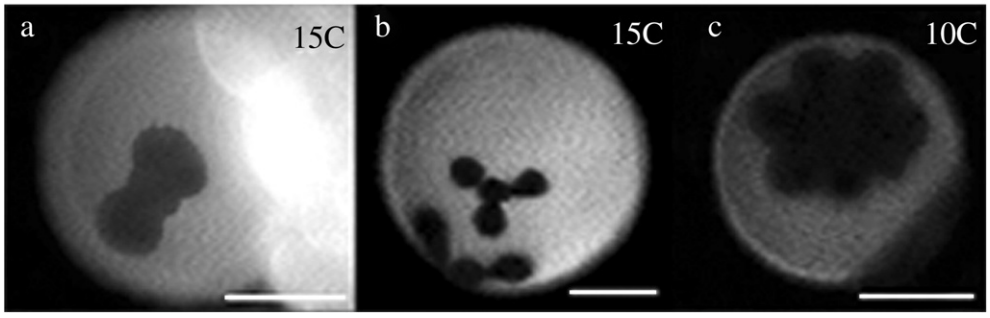

Fig. 7. Phase separation in a quaternary EPC/ESM/ECER/CHOL 50/30/10/10 mixture. The number of petals decreases to two or tree at 15–20 °C (a and b). The dark leaf-like domains display a large round-shaped central area with small petal dimensions (c). Bar 20 μm.

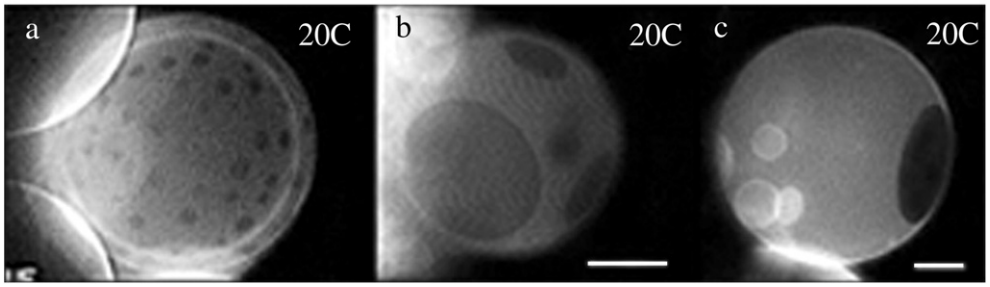

Fig. 8. Phase separation in a ternary EPC/ESM/CHOL 65/17.5/17.5 raft mixture (a) compared to quaternary EPC/ESM/ECER/CHOL 60/17.5/5/17.5. Raft separation is prompted by 5% ceramide (b) as compared to ternary EPC/ESM/CHOL 60/22.5/17.5 mixture in which sphingolipid content is preserved at 22.5% (c). The comparison demonstrates the large increase in the dark areas assigned to the liquid-ordered phase for ceramide-containing quaternary mixture (b) compared to control mixtures (a and c). Bar 20 μm.

prepared from EPC/ESM/CHOL 60/22.5/17.5 mixtures with sphingomyelinase (Fig. 11). The lipid ratio EPC/ESM/CHOL 65/17.5/17.5 was modified to avoid L_o/L_d phase transition at 20 °C and to obtain a large dark fraction for better visualization of the progress of enzyme hydrolysis. The injection of the enzyme adjacent to the external membrane surface took approximately 5 s and enabled the space around the vesicle to be saturated with sphingomyelinase. In accordance with the results reported by Taniguchi et al. [32] as well as our own observations, the data showed that sphingomyelinase activity did not maintain an L_o domain entity. The SM to CER conversion resulted in the following macroscopically-resolved stages during the time course of enzymic activity:

1) Fusion of L_o domains where more than one domain exists (Fig. 11a–c).
2) Appearance of noticeable L_o border undulations.
3) Loss of circular L_o domains and appearance of elongated forms (Fig. 11c).
4) Disintegration of L_o domains and subsequent reorganization of membrane phases, transformation of L_o/L_d phase separation into L_β/L_d. Formation of irregular dark domains in the form of a narrow channel on the bright background (Fig. 11d and e).
5) Membrane invagination or vesicle collapse upon addition of more enzyme.
6) Reorganization of the dark fraction and formation of leaf-like gel domains with two or three petals at low temperatures (4 °C) (Fig. 11f). The phase morphology appears like phase separation in an EPC/ESM/ECER/CHOL 50/30/10/10 quaternary mixture at low temperatures inferring that the SM/CER ratio is approximately 3/1 in a mixture of proportions of which are dynamically controlled by sphingomyelinase. However, this situation is unusual and likely to be defined by the initial lipid ratio of the ternary mixture and the final ratio of the quaternary mixture resulting from enzyme-induced SM degradation.

Briefly, the formation of CER from SM induced by sphingomyelinase caused destabilization and disintegration of the L_o domains. Liquid-ordered phase presented as circular domains were gradually converted into gel phase during the enzyme treatment. In cases when the ESM content was large enough (EPC/ESM/CCHOL 45/45/10), sphingomyelinase activity on a L_o/L_d membrane at 37 °C induced initially a bright L_d invagination and small vesicle-budding, which did not allow further clear detection of L_o domains by the epifluorescence method (data not shown). This result was not unexpected because Holopainen et al. [33] have reported similar invaginations in phosphatidylcholine/sphingomyelin GUV membranes. Apparently, in EPC/ESM/CHOL 45/45/10 mixture, the L_d phase (bright region) was highly enriched in ESM and this bright region, already enriched in ceramide due to sphingomyelinase action, was more susceptible to inward curvatures compared to the stiff L_o phase.

3.5. Phospholipase A_2 activity in a L_o/L_d heterogeneous membrane

The activity of $sPLA_2$ on GUVs prepared from pure EPC, serving as enzyme substrate, was characterized by disturbance of membrane integrity. Only 5 s after the enzyme injection total vesicle fragmentation was observed by formation of small vesicles (Supplementary data, Fig. 1). A wide variety of discontinuous vesicle shapes and

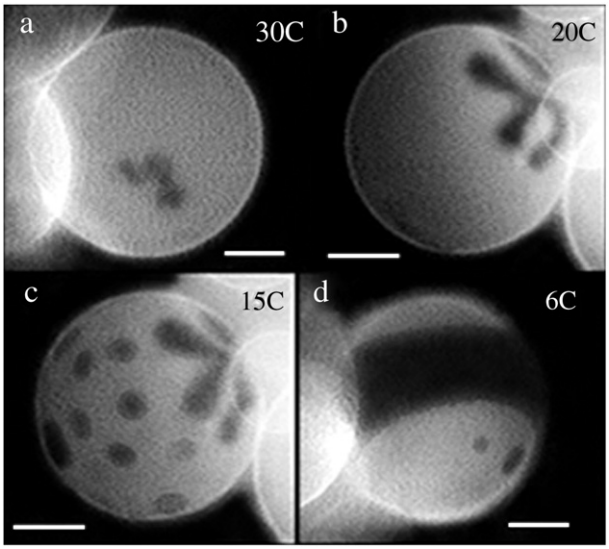

Fig. 9. Phase separation changes with temperature for quaternary EPC/ESM/ECER/CHOL 50/17.5/15/17.5 mixture. Dark irregular domains are visualized at 30 °C (a), leaf-like domains at 20 °C (b), round-shaped domains at 15 °C and band-like domains at low temperatures (d). The observation of dark leaf-like and round-shaped domains is consistent with $L_\beta/L_o/L_d$ phase coexistence at 15 °C for this composition (c). Bar 20 μm.

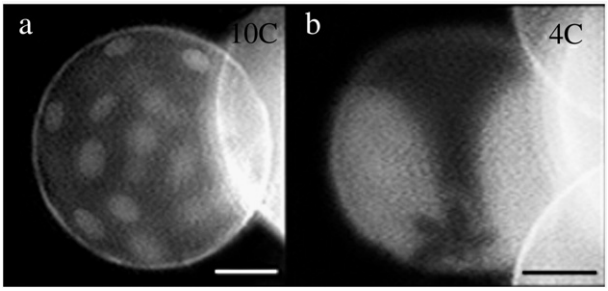

Fig. 10. Phase separation in quaternary EPC/ESM/ECER/CHOL 45/17.5/20/17.5 mixture. Formation of many small bright domains is detected at 10 °C on a dark background (a). Visualization of domains with three different shapes (dark leaf-like and band, bright areas) is consistent with $L_\beta/L_o/L_d$ phase coexistence at low temperatures for this quaternary mixture (b). Bar 20 μm.

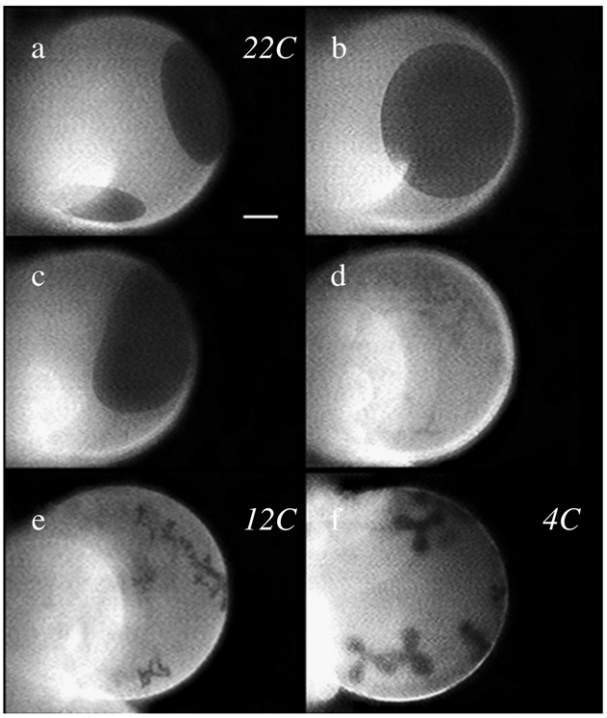

Fig. 11. Hydrolysis of sphingomyelin by sphingomyelinase in heterogeneous L_o/L_d membrane of GUVs prepared of EPC/ESM/Chol (60/22.5/17.5) at 22 °C. L_o/L_d phase visualization (a). L_o domain fusion after enzyme micro-injection (b). After 5 to 10 min, appearance of significant L_o border undulations, loss of round-shaped L_o domains and formation of elongated domains was detected (c). L_o domain disintegration and formation of irregular dark domains occurs between 10 and 20 min after the enzyme injection (d). Leaf-like domain formation with two, three or four petals is observed at lower temperatures (e and f). The same vesicle is presented in the series of images. Bar 20 μm.

topology transformations were observed upon varying the amount of enzyme and vesicle lipid composition (Supplementary data, Fig. 2) [34,35]. In contrast, $sPLA_2$ treatment of EPC/ESM 1/1 GUVs did not induce significant transformations in vesicle shape where no apparent macroscopic phase separation was detected at 37 °C (Supplementary data, Fig. 3). Only slight vesicle shrinking, resulting from partial hydrolysis, was observed. This process, however, was rapidly terminated and the vesicles retained their initial shape. Apparently, the presence of SM in the model membranes augmented membrane resistance to $sPLA_2$. This could be attributed to the inhibitory effect of SM on this enzyme. When a small fraction of ESM (2%) was replaced with ECER, a rapid rate of substrate hydrolysis was initiated on exposure to PLA_2 manifest by appearance of a hole in the membrane bilayer and a sharp reduction in vesicle diameter (Supplementary data, Fig. 4). Obviously in this case the reaction did not proceed at the same rate as in GUVs of EPC (about 5 s), but still an almost complete hydrolysis of substrate was observed in about 28 s. Vesicle rupture was observed when 5%ESM was replaced by 5%ECER.

In control "raft" EPC/ESM/CHOL 45/45/10 mixture $sPLA_2$ activity induced *continuous* L_o domain budding and fission without appearance of holes or L_d membrane fragmentation (Fig. 12A) as has been shown in our previous work [24]. When the cholesterol content was augmented in ternary mixtures, increasing amounts of SM was engaged in the dominant SM/CHOL interactions resulting in an increase of L_o domain formation. In contrast, the L_d phase became more SM-depleted. Thus the presence of CHOL relieved the inhibitory effect of the latter [36] and the L_d phase became more susceptible to PLA_2 hydrolysis. Similar effects could be achieved when only 2%ESM was replaced by ECER in the EPC/ESM/ECER/CHOL (45/43/2/10) mixture leading to a complete L_d phase fragmentation (Fig. 12B). The same L_d phase remained intact in the control mixture (EPC/ESM/CHOL 45/45/10) [24].

The budding process in EPC/ESM/ECER/CHOL (45/43/2/10) mixture was triggered within 1 s after $sPLA_2$ injection (Fig. 12B, c) whereupon it developed (Fig. 12B, d and e) and was finalized after about 4 s by fission of raft-like liquid-ordered domains (Fig. 12B, f). These experiments demonstrated the role of CER as a powerful activator of the $sPLA_2$ activity, manifested by rapid transformation of the vesicle membrane bilayer into small vesicles (Fig. 12B, f–i). The L_d phase was completely disintegrated after 16 s (Fig. 12B i) in contrast to the L_o phase, which remained intact. Briefly, both CER and CHOL acted as phospholipase A_2 activators due to their predominant interactions

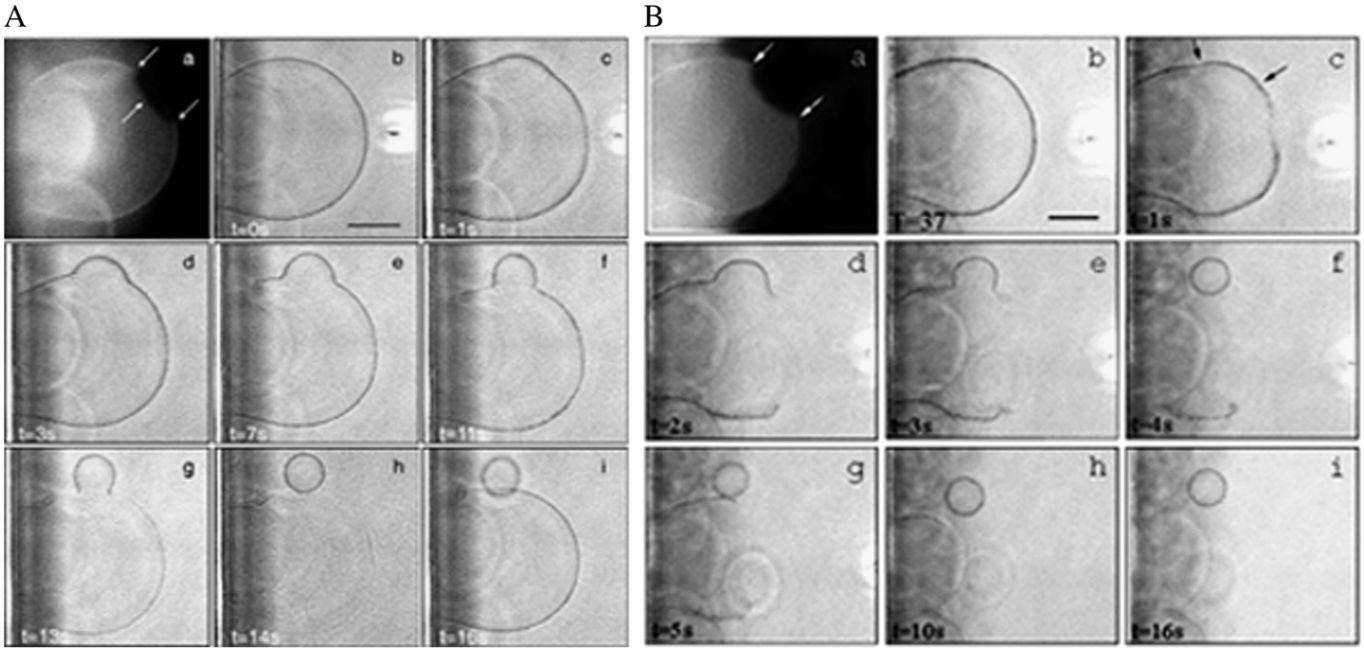

Fig. 12. $sPLA_2$ activity in control "raft" EPC/ESM/CHOL 45/45/10 mixture induces *continuous* L_o domain budding and fission (A), published in Staneva et al. [24]. $sPLA_2$ activity in EPC/ESM/ECER/CHOL 45/43/2/10 mixture (B). One second after $sPLA_2$ injection, the budding process triggeres (B, c), develops (B, d and e) and after about 4 s finalizes by fission of raft-like liquid-ordered domain (B, f). L_d phase is completely disintegrated for 16 s (B, f–i) in contrast to the L_o phase which remains intact. The same vesicle is presented in the series of images. Bar 20 μm.

with SM, thus making the phospholipid substrate more susceptible for enzyme hydrolysis.

4. Discussion

In this work we investigated the mechanism of CER-induced modulation of SM/CHOL domain formation with respect to the changes in the domain form, size and dynamics. It is well known that the liquid-ordered phase is organized in the membrane plane as a large number of perfectly round domains embedded in a fluid environment. Domains grow in size by fusion with other domains and they quickly return to a circular shape to minimize line tension by optimizing the area-to perimeter ratio [28,29,37]. The initial studies were of binary mixtures of EPC/ECER (the latter being up to 20%). These mixtures exhibit gel/liquid phase coexistence as shown by X-ray and ESR methods [16]. This phase separation is well resolved in GUV membranes as a few dark, leaf-like domains on a bright background (Fig. 1). The shape of the leaf-like domains was governed more by long-range electrostatic repulsion between the lipid dipoles than by the line tension, which would also explain why fusion between leaf-like domains was never observed in our experiments. The electrostatic repulsive forces tend to maximize the distance between molecules within a domain and thus favor less densely packed, irregular or fractal-like domains [38,39]. Domains with similar shapes and properties have been previously visualized in binary mixtures but they were composed of different lipid species, characterized by different length and saturation of the fatty acids. For example, such domains were detected in dimyristoyl-PC/C24:1-CER mixtures but not in dimyristoyl-PC/C16:0-CER using monomolecular films [40], in bovine brain SM/CER mixtures [15] as well as in ESM/ECER mixtures containing 30% CER [41] and palmitoyl-oleoyl-PC/brain CER [42]. We have observed that there is a difference in CER gel domain formation between mono-, bi-molecular films and free-standing GUVs. This difference is in the formation of lateral superstructure organization including five or six nearest-neighbor [15,43] in monomolecular films and the formation of a single or few leaf-like domains, line-bound like a necklace in GUVs. Curvature constraints could be one reason for the lack of lateral superstructure organization in vesicles. On the other hand, however, there is a difference in the domain shape between palmitoyl-oleoyl-PC/brain CER and EPC/ECER mixtures in free-standing GUVs. In the former, increasing proportions of CER leads to formation of domains with a stripe-like appearance [42] but such shapes were never observed in the latter. The preferred domain shape that was resolved in EPC/ECER binary mixtures was leaf-like. A likely explanation of this disparity could be either the different nature of the lipid species comprising the vesicle or insufficient resolution to observe such narrow domains at high temperatures under our experimental conditions.

The presence of cholesterol in this series of EPC/ECER/CHOL ternary mixtures (80/10/10, 70/10/20, 60/10/30), induced a dramatic decrease in the phase transition temperature compared to that in a EPC/ECER 90/10 binary mixture (T_m=42 °C). From X-ray diffraction results, T_m was reduced by 8 °C with1/2 CER/CHOL ratio and by 16 °C with a 1/3 molar ratio [16]. This effect of CHOL is obvious in GUVs where in the presence of low proportions of CHOL (1/1 CER/CHOL) leaf-like gel domains could still be recognized at the same temperatures (Fig. 2), whereas with higher proportions of CHOL this could no longer be seen (Fig. 3). Instead, a few small dark domains were observed at low temperatures. In addition, fusion of these domains has never been observed even with high proportions of CHOL over a long period indicating that the quasi-round dark domains at 30% CHOL are typical gel domains and EPC/ECER/CHOL ternary mixtures do not exhibit liquid/liquid immiscibility in the same form as L_o/L_d. Obviously, CER and CHOL are not involved in the organization of liquid-ordered phase of the type formed by SM and CHOL. The specific ability of liquid domains to fuse is precisely the property that allows visualization of phase separation on the micron scale. ESR data in our recent paper showed that an increase in the proportion of CHOL is associated with a significant increase of the molecular order parameter for the liquid-disordered phase [16]. Apparently, CHOL induces higher miscibility of CER in glycerophospholipid/ceramide mixtures which could explain the shifting in leaf-like domain formation to lower temperatures and the gradual decrease of the gel dark fraction upon augmentation of CHOL content. In accordance with this idea, Fidorra et al. [42] reported an ordering effect of CHOL on more fluid regions of the membrane diminishing the extent of water dipolar relaxation phenomena around a laurdan fluorescent probe.

The presence of sphingomyelin in a proportion of only 5% in EPC/ESM/ECER/CHOL quaternary mixtures induced re-appearance of the gel phase in the entire temperature range from 2° to 46 °C [16]. X-ray and ESR spectroscopy data showed that in quaternary mixtures SM not only stabilizes the gel phase but the molecular order parameter of the chains in gel phase was also increased. Such specific interactions between CER and SM are also supported by the report that bovine brain SM forms a gel-phase complex with CER from the same source [17]. Thus it was shown that CER competes with CHOL for SM, a notion first proposed by London and London [12]. A gradual increase of the SM content (20%, 30%) in the first series of quaternary mixtures leads to three-phase coexistence ($L_\beta/L_o/L_d$) according to X-ray and ESR data [16]. The visualization of this three-phase coexistence and more precisely of the L_o phase is obvious in Figs. 6 and 9 where dark circular domains, characterized by their ability to fuse, were observed. The coexistence of gel phase with a liquid-ordered phase implies that SM also interacts with CHOL, thereby preventing CHOL from destabilizing the CER-enriched gel phase. Surprisingly, on a micron scale, at temperatures below 30 °C, the variations in the form of the leaf-like domains were sensitive to the proportion of SM in the mixture. Higher proportions of SM content was accompanied by a transition from domain shape with high rotation symmetry as leaf-like domains with 6–9 petals to lower ones with 2–3 petals or quasi-circular domain shape. This transition in domain shape could reflect the formation of a new CER/SM gel phase. Similar results have been obtained by Maggio's group [15,43] where CER content increases gradually in a simple SM monolayer membrane by either sphingomyelinase action or pre-defined SM/CER mixtures but the shape transition is reversed from circular to fractal-like domains. The second series of quaternary mixtures (EPC/ESM/ECER/CHOL) was chosen as a model of plasma membranes which typically contain about 15–40% CHOL and 10–30% SM. The main purpose was to show how phase morphology of pre-defined L_o/L_d mixtures was changed in the presence of CER as well as to clarify the role of CER in the formation of such complex lateral heterogeneity. Addition of only 5% of ECER to the control mixture containing 65/17.5/17.5 EPC/ESM/CHOL was associated with the appearance of L_β, phase in the entire temperature range. This contrasts with the behavior of the ternary mixture in the absence of ECER in which coexistence of only L_o/L_d phases were observed according X-ray and ESR data [16]. Interestingly, in the presence of up to 10% ECER, gel phase was not visualized by fluorescence unlike the L_o phase which was clearly observed (Fig. 10). The round shape of the dark domains and their ability to fuse were preserved for these CER ratios. The fact that the dark fractions are increased implies that CER participates in the dark domain structures and yet their liquid-like state was preserved. It is noteworthy that the identification of gel phase within L_o domains has recently been reported in GUVs using a combination of three fluorescent probes [44]. Higher CER concentrations (15%, 20%) induced formation of a gel phase (dark irregular domains, Fig. 11) at higher temperatures compared to EPC/ECER 90/10 and EPC/ECER/CHOL 80/10/10 mixtures (Figs. 1 and 2). However, at lower temperatures formation of L_o phase was observed (Figs. 9a and 10c) compared to control EPC/ESM/CHOL 65/17.5/17.5 mixture (Fig. 8a). Further CER augmentation leads to phase percolation characterized by dark fraction domination (Fig. 10).

These experiments clearly demonstrate that CER and CHOL compete in their interaction with SM. CER in quaternary mixtures is associated with and is responsible for the formation of a CER/SM highly ordered gel phase which could explain the appearance of the gel phase at higher temperature unlike pure CER gel phase in EPC/ECER binary mixtures. Thus, less SM is engaged in SM/CHOL interactions which could explain the L_o domain formation at lower temperatures compared to control EPC/ESM/CHOL ternary mixture. Finally, some CHOL could be released for the L_d phase. Briefly, we can conclude that CER governs lipid interactions and arrangements in PC/SM/CER/CHOL quaternary mixtures.

One other important question is how a L_o/L_d heterogeneous membrane, with microdomains in the membrane plane, is reorganized and dynamically controlled by an enzyme activity, after CER generation and accumulation (Fig. 11). It was demonstrated that sphingomyelinase activity does not maintain L_o domain entity and the morphology of the coexisting phases is completely altered. Circular domains of L_o phase were transformed into dark narrow channel-like domains on the bright background during the first 20–30 min of SM conversion into CER and these domains were stable at least for 1 h after their formation. The structural organization of these gel domains was not clearly resolved. For example, lower temperatures allowed us to identify certain regular structure: formation of necklace of three-petal leaf-like domains at 4 °C. It should be mentioned that in this case the lipid system is out of thermodynamic equilibrium because of continuous enzyme activity and asymmetric generation of CER in comparison with the pre-defined mixtures. The processes of membrane reorganization are controlled by the lateral and transverse diffusion of the lipids at the time scale of our experiment. It is known that CER has a comparatively rapid flip-flop movement compared with other lipids (half-time of 22 min at 37 °C for fluorescent analogue of CER [20] and half-time of approximately 1 min at the same temperature for unlabeled-C16 CER [19]). Despite the rapid flip-flop of CER, it is difficult to make some comparisons between dynamically controlled lipid systems, which are out of equilibrium because of continuous asymmetric CER generation and pre-defined mixtures in thermodynamic equilibrium.

These results show convincingly how CER could dramatically change the phase morphology of heterogeneous membranes. As demonstrated by our results, CER is characterized by a high immiscibility with other lipids. Glycerophospholipid/ceramide mixtures exhibit liquid/gel immiscibility. CHOL readily melts CER in a glycerophospholipid environment while SM stabilizes the gel phase and thus decreases CER miscibility. Specific CER/SM interactions induce a change in the conditions of L_o phase formation (SM/CHOL interactions). This complex CER immiscibility in pre-defined and dynamically controlled by enzyme activity "raft" mixtures encouraged revision of the simple comparison that is often made between the biophysical definition of "rafts", i. e. liquid-ordered phase (enriched in SM and CHOL) and the more complex and biologically relevant conception of membrane "rafts". Thus a relatively small amount of CER induced gel phase formation, particularly in the SM environment, dramatically altering the domain shape, size and their intrinsic properties such as dynamics and fusion. Direct incorporation of CER in ternary *raft* mixtures (about 20% CHOL) induced significant dark phase enlargement (Fig. 8a and b). Surprisingly, this dark phase preserved its liquid-like property even at high CER content. This result supports the studies hypothesized that CER can promote the formation of large signaling platforms if this concerns micron scale. However, the enzyme generation of CER did not maintain micron L_o domains, the existence of smaller domains cannot be excluded, and instead the formation of gel-like domains is observed (Fig. 11b–d). One reason for this could be the critical SM concentration, which is not sufficient for L_o domain formation, even at low temperatures under our experimental conditions. Another reason could be insufficient resolution provided by the fluorescence method. Studies on a nanometer scale, using atomic force microscopy, resolved the substructure of these micron patches [45]. The domains have two distinct heights (assigned to L_β and L_o phase) and are usually clustered together imbedded in the surrounding lower phase (L_d). The observed micron gel-like cluster in our studies moved as an entity, which is in accordance with this data.

The presence of relatively low proportions of CER induces significant morphological vesicle transformations after $sPLA_2$ treatment unlike PC/SM vesicles. It should be noted that the vesicle response was not only due to the enzyme activity but also to the membrane elasticity of the vesicle. Nevertheless, a correlation was established between the enzyme activity and the vesicle morphological transformations. The exact mechanism of the observed $sPLA_2$ activation by CER is still unknown. The consensus opinion is that this activation is due to formation of gel microdomains when the concentration of CER is at least 5% [46–48]. Our present studies (Fig. 12) as well as the results reported by Koumanov at al. [22] showed that this activation occurs even at 2% CER. It was presumed that CER up to 2% is not sufficient to form microdomains but CER molecules serve as a nucleation sites for enzyme insertion into the substrate bilayer. However, in SM-enriched mixtures, SM tends to stabilize these domains by formation of stable complexes with CER. Thus, CER like cholesterol sequestrates SM, a $sPLA_2$ inhibitor, making the phospholipid substrate more susceptible to enzyme attack. Two patches are formed in the membrane bilayer: substrate and non-substrate sites unlike a homogeneous PC/SM membrane. Cohesive forces in homogeneous membranes, even after substrate hydrolysis, are apparently stronger compared to heterogeneous membranes (PC/SM/CER or PC/SM/CER/CHOL) where substrate patches are converted into products (lysophosphatidylcholine and fatty acid). The tensile strength (cohesive forces) of the membrane decreases with increasing lysophosphatidylcholine concentration [49,50]. This decrease in the membrane strength determines the substantial decrease in the necessary work for membrane breakdown. For example an increase in the lysophosphatidylcholine concentration above 50 mol% results in an apparent disappearance of the spontaneously formed bilayer structures and their replacement by micellar structures. Thus, these results demonstrate how CER could modulate $sPLA_2$ activity and the processes such as membrane fragmentation, budding in and budding out by inducing changes in the phase state of the lipid bilayer.

4.1. Cellular implications

As mentioned in the Introduction, the presence of CER in glycerophospholipid liposomes leads to enhancement of PLA_2 hydrolytic activity [22]. This is attributed to membrane defects caused by different bilayer thickness of the coexisting phases. Our current results reveal that CER in binary, ternary and quaternary mixtures forms gel domains over a wide temperature range. The inter-phase is precisely where membrane defects appear and where phospholipases A_2 [51] and sphingomyelinases [45] are highly active. We have established in our previous studies, that in mixtures of PC/SM or PC/SM/PE/PS, sphingomyelin inhibits PLA_2 activity [36–52]. Pre-treatment of phosphatidylcholine/sphingomyelin liposomes with sphingomyelinase leads to increased PLA_2 activity [22]. Thus, it is possible that the generated ceramide segregates into complex gel-like microdomains which underlie the formation of membrane defects, occurring as a prerequisite for augmentation of the enzyme activity. It is also possible that CER/SM interactions dominate over those of SM/CHOL, thus CER sequestrates SM, making the glycero-phospholipid substrate more susceptible for the PLA_2 hydrolysis. At a cellular level the events probably follow the same model because a similar behavior is reproduced upon treatment of CHO-2B cells with sphingomyelinase [22,53]. It is known that the activation of this enzyme, due to different stress factors for example, precedes PLA_2 activation. We assume that this intrinsic capacity of CER could make it a potential modulator of PLA_2 activity in cells. As shown here and in our previous work, PLA_2 activity in heterogeneous membranes induces morphological process such as membrane fragmentation, budding in [33] and

budding out [24]. In addition, it was reported that PLA_2 is a mediator of membrane shape and function in membrane trafficking [54]. It was also proposed that ceramide-enriched membrane platforms are ideal structures to sort proteins in cells and to provide a mean for the spatial re-organization of receptors [55]. By these molecular mechanisms CER might exercise its role in cell signaling and trafficking.

Acknowledgements

The authors are grateful to C. Tessier and P. Nuss for the many enlightening discussions. The work was aided by grants from Bulgarian Ministry of Education and Science, National Programme for Development of Scientific Potential and the Human Frontier Science Program (RGP0016/2005).

Appendix A. Supplementary data

Supplementary data associated with this article can be found, in the online version, at doi:10.1016/j.bbamem.2008.10.026.

References

[1] Y.A. Hannun, Functions of ceramide in coordinating cellular responses to stress, Science 274 (1996) 1855–1859.
[2] S. Manes, A. Viola, Lipid rafts in lymphocyte activation and migration (review), Mol. Membr. Biol. 23 (2006) 59–69.
[3] J.F. Hancock, Lipid rafts: contentious only from simplistic standpoints, Nat. Rev. Mol. Cell Biol. 7 (2006) 456–462.
[4] A. Morales, H. Lee, F.M. Goni, R. Kolesnick, J.C. Fernandez-Checa, Sphingolipids and cell death, Apoptosis 12 (2007) 923–939.
[5] S. Chiantia, N. Kahya, H. Ries, P. Schwille, Effects of ceramide on liquid-ordered domains investigated by simultaneous AFM and FCS, Biophys. J. 90 (2006) 4500–4508.
[6] I. Johnston, L. Johnston, Ceramide promotes restructuring of model raft membranes, Langmuir (2006) 11284–11289.
[7] E.L. Laviad, L. Albee, I. Pankova-Kholmyansky, S. Epstein, H. Park, A.H. Merril, A.H. Futerman, Characterization of ceramide synthase 2 — tissue distribution, substrate specificity, and inhibition by sphingosine 1-phosphate, J. Biol. Chem. 283 (2008) 5677–5684.
[8] T. Levade, J.P. Jaffrezou, Signalling sphingomyelinases: which, where. how and why? Biochim. Biophys. Acta 1438 (1999) 1–17.
[9] R.J. Veldman, N. Maestre, O.M. Aduib, J.A. Medin, R. Salvayre, T. Levade, A neutral sphingomyelinase resides in sphingolipid-enriched microdomains and is inhibited by the caveolin-scaffolding domain: potential implications in tumour necrosis factor signalling, Biochem. J. 355 (2001) 859–868.
[10] P.S. Liu, R.G.W. Anderson, Compartmentalized production of ceramide at the cell-surface, J. Biol. Chem. 270 (1995) 27179–27185.
[11] A. Cremesti, F. Paris, H. Grassme, N. Holler, J. Tschopp, Z. Fuks, E. Gulbins, R. Kolesnick, Ceramide enables Fas to cap and kill, J. Biol. Chem. 276 (2001) 23954–23961.
[12] M. London, E. London, Ceramide selectively displaces cholesterol from ordered lipid domains (rafts): implications for raft structure and function, J. Biol. Chem. 279 (2004) 9997–10004.
[13] M.P. Veiga, J.L. Arrondo, F.M. Goni, A. Alonso, Ceramides in phospholipid membranes: effects on bilayer stability and transition to nonlamellar phases, Biophys. J. 76 (1999) 342–350.
[14] R.N. Kolesnick, F.M. Goni, A. Alonso, Compartmentalization of ceramide signaling: physical foundations and biological effects, J. Cell. Physiol. 184 (2000) 285–300.
[15] S. Hartel, M.L. Fanani, B. Maggio, Shape transitions and lattice structuring of ceramide-enriched domains generated by sphingomyelinase in lipid monolayers, Biophys. J. 88 (2005) 287–304.
[16] G. Staneva, C. Chachaty, C. Wolf, K. Koumanov, P. J. Quinn, The role of sphingomyelin in regulating phase coexistence in complex lipid model membranes: competition between ceramide and cholesterol, Biochim. Biophys. Acta 1778 (2008) 2727–2739.
[17] J.B. Massey, Interaction of ceramides with phosphatidylcholine, sphyngomyelin and sphyngomyelin/cholesterol bilayers, Biochem. Biophys. Acta 1510 (2001) 167–184.
[18] A. Helvoort, G. van Meer, Intracellular lipid heterogeneity caused by topology of synthesis and specificity in transport. Example: sphingolipids, FEBS Lett. 369 (1995) 18–21.
[19] I. Lopez-Montero, N. Rodriguez, S. Cribier, A. Pohl, M. Velez, P. Devaux, Rapid transbilayer movement of ceramides in phospholipid vesicles and in human erythrocites, J. Biol. Chem. 280 (2005) 25811–25819.
[20] J. Bai, R.E. Pagano, Measurement of spontaneous transfer and transbilayer movement of BODIPY-labeled lipids in lipid vesicles, Biochemistry 36 (1997) 8840–8848.
[21] F.-X. Contreras, A.-V. Villar, A. Alonso, R.N. Kolesnick, F.M. Goni, Sphingomyelinase activity causes transbilayer lipid translocation in model and cell membranes, J. Biol. Chem. 278 (2003) 37169–37174.
[22] K.S. Koumanov, A.B. Momchilova, P.J. Quinn, C. Wolf, Ceramides increase the activity of the secretory phospholipase A2 and alter its fatty acid specificity, Biochem. J. 363 (2002) 45–51.
[23] M. Angelova, D. Dimitrov, Liposome electroformation, Faraday Discuss. Chem. Soc. 81 (1986) 303–311.
[24] G. Staneva, M.I. Angelova, K. Koumanov, Phospholipase A2 promotes raft budding and fission from giant liposomes, Chem. Phys. Lipids 129 (2004) 53–62.
[25] S.L. Veatch, I.V. Polozov, K. Gawrisch, S.L. Keller, Liquid domains in vesicles investigated by NMR and fluorescence, Biophys J. 86 (2004) 1922–2910.
[26] R.M. Weis, H.M. McConnell, Cholesterol stabilizes the crystal–liquid interface in phospholipid monolayers. J. Phys. Chem. 89 (1985) 4453–4459.
[27] M. Ruano, K. Nag, L. Worthman, C. Casals, J. Perez-Gil, K. Keough, Differential partitioning of pulmonary surfactant protein SP-A into regions of monolayers of dipalmitoylphosphatidylcholine and dipalmitoylphosphatidylcholine/dipalmitoylphosphatidylglycerol, Biophys. J. 74 (1998) 1101–1109.
[28] C. Dietrich, L.A. Bagatolli, Z.N. Volovyk, N.L. Tompson, M. Levi, K. Jacobson, E. Gratton, Lipid rafts reconstituted in model membranes. Biophys. J. 80 (2001) 1417–1428.
[29] T. Baumgart, S.T. Hess, W.W. Webb, Imaging coexisting fluid domains in biomembrane models coupling curvature and line tension, Nature 425 (2003) 821–824.
[30] K. Bacia, P. Schwille, T. Kurzchalia, Sterol structure determines the separation of phases and the cuvature of the liquid-ordered phase in model membranes, Proc. Natl. Acad. Sci. 102 (2005) 3272–3277.
[31] E. Gulbins, R. Kolesnick, Acid sphingomyelinase-derived ceramide signaling in apoptosis, Subcell. Biochem. 36 (2002) 229–244.
[32] Y. Taniguchi, T. Ohba, H. Miyata, K. Ohki, Rapid phase change of lipid microdomains in giant vesicles induced by conversion of sphingomyelin to ceramide, Biochim. Biophys. Acta 1758 (2006) 145–153.
[33] J.M. Holopainen, M. Angelova, P.K.J. Kinnunen, Vectorial budding of vesicles by asymmetrical enzymatic formation of ceramide in giant liposomes, Biophys. J. 78 (2000) 830–838.
[34] R. Wick, M.I. Angelova, P. Walde, P.L. Luisi, Microinjection into giant vesicles and light microscopy investigation of enzyme-mediated vesicle transformations, Chem. Biol. 3 (1996) 105–111.
[35] S.A. Sanchez, L.A. Bagatolli, E. Gratton, T.L. Hazlett, A two-photon view of an enzyme at work: *Crotalus atrox* venom PLA2. Interaction with single-lipid and mixed-lipid giant unilamellar vesicles, Biophys. J. 82 (2002) 2232–2243.
[36] K.S. Koumanov, P.J. Quinn, G. Bereziat, C. Wolf, Cholesterol relieves the inhibitory effect of sphingomyelin on type II secretory phospholipase A2, Biochem. J. 336 (1998) 625–630.
[37] S.L. Veatch, S.L. Keller, Separation of liquid phases in giant vesicles of ternary mixtures of phospholipids and cholesterol, Biophys. J. 85 (2003) 3074–3083.
[38] H.M. McConnel, Harmonic shape transitions in lipid monolayer domains, J. Phys. Chem. 94 (1990) 4728–4731.
[39] K.Y.C. Lee, H.M. McConnell, Quantized symmetry of liquid monolayer domains, J. Phys. Chem. 97 (1993) 9532–9539.
[40] J.M. Holopainen, H.L. Brockman, R.E. Brown, P.K.J. Kinnunen, Interfacial interactions of ceramide with dimyristoylphosphatidylcholine: impact of the N-acyl chain, Biophys. J. 80 (2001) 765–775.
[41] J. Sot, L.A. Bagatolli, F.M. Goni, A. Alonso, Detergent-resistant, ceramide-enriched domains in sphingomyelin/ceramide bilayers, Biophys. J. 90 (2006) 903–914.
[42] M. Fidorra, L. Duelund, C. Leidy, A.C. Simonsen, L.A. Bagatolli, Absence of fluid-ordered/fluid-disordered phase coexistence in ceramide/POPC mixtures containing cholesterol, Biophys. J. 90 (2006) 4437–4451.
[43] M.L. Fanani, S. Hartel, R. Oliveira, B. Maggio, Bidirectional control of sphingomyelinase activity and surface topography in lipid monolayers, Biophys. J. 83 (2002) 3416–3424.
[44] J. Sot, M. Ibarguren, J.V. Busto, L.-R. Montes, F.M. Goni, A. Alonso, Cholesterol displacement by ceramide in sphingomyelin-containing liquid-ordered domains, and generation of gel regions in giant lipidic vesicles, FEBS Lett. 532 (2008) 3230–3236.
[45] I. Johnston, L. Johnston, Sphingomyelinase generation of ceramide promotes clustering of nanoscale domains in supported bilayer membranes, Biochim. Biophys. Acta 1778 (2008) 185–197.
[46] J.W. Huang, E.M. Goldberg, R. Zidovetzki, Ceramide reduces structural defects in phosphatidylcholine bilayers and activates phospholipase A2, Biochem. Biophys. Res. Commun. 220 (1996) 834–838.
[47] J.M. Holopainen, J.Y.A. Lehtonen, P.K.J. Kinnunen, Lipid microdomains in dimyristoylphosphatidylcholine/ceramide liposomes, Chem. Phys. Lipids 88 (1997) 1–13.
[48] J.M. Holopainen, M. Subramanian, P.K.J. Kinnunen, Sphingomyelinase induces lipid microdomains formation in fluid phosphatidylcholine/sphingomyelin membrane, Biochemistry 37 (1998) 17562–17570.
[49] D. Needham, R.S. Nunn, Elastic deformation and failure of lipid bilayer membranes containing cholesterol, Biophys. J. 58 (1990) 997–1009.
[50] D.V. Zhelev, Material property characteristics for lipid bilayers containing lysolipid, Biophys. J. 75 (1998) 321–330.
[51] M. Grandbois, H. Clausen-Schaumann, H. Gaub, Atomic force microscope imaging of phospholipid bilayer degradation by phospholipase A2, Biophys. J. 74 (1998) 2398–2404.
[52] K. Koumanov, C. Wolf, G. Bereziat, Modulation of human type II secretory phospholipase A2 by sphingomyelin and annexin VI, Biochem. J. 326 (1997) 227–233.
[53] E. Klapisz, J. Masliah, G. Bereziat, C. Wolf, K.S. Koumanov, Sphingolipids and cholesterol modulate membrane susceptibility to cytosolic phospholipase A2, J. Lipid Res. 41 (2000) 1680–1688.
[54] W.J. Brown, K. Chambers, K.A. Doody, Phospholipase A2 (PLA2) enzymes in membrane trafficking: mediators of membrane shape and function, Traffic 4 (2003) 214–221.
[55] Y. Zhang, X. Li, K.A. Becker, E. Gulbins, Ceramide-enriched membrane domains-Structure and function, Biochim. Biophys. Acta, doi:10.1016/j.bbamem.2008.07.030.